

Supporting Information for:

## Formation of polysulfides as a smart strategy to selectively detect H<sub>2</sub>S in a Bi(III)-based MOF material

Valeria B. López-Cervantes,<sup>a†</sup> Juan L. Obeso,<sup>a,b†</sup> J. Gabriel Flores,<sup>c,d†</sup> Aída Gutiérrez-Alejandre,<sup>e</sup> Raul A. Marquez,<sup>f</sup> José Antonio de los Reyes,<sup>d</sup> Catalina V. Flores,<sup>a,b</sup> N. S. Portillo-Vélez,<sup>g</sup> Pablo Marín-Rosas,<sup>g</sup> Christian A. Celaya,<sup>h</sup> Eduardo González-Zamora,<sup>g</sup> Diego Solis-Ibarra,<sup>\*a</sup> Ricardo A. Peralta<sup>\*g</sup> and Ilich A. Ibarra<sup>\*a,i</sup>

---

<sup>a.</sup> *Laboratorio de Físicoquímica y Reactividad de Superficies (LaFReS), Instituto de Investigaciones en Materiales, Universidad Nacional Autónoma de México, Circuito Exterior s/n, CU, Coyoacán, 04510, Ciudad de México, México. Ilich A. Ibarra: Email: argel@unam.mx*

<sup>b.</sup> *Instituto Politécnico Nacional, CICATA U. Legaria, Laboratorio Nacional de Ciencia, Tecnología y Gestión Integrada del Agua (LNAgua), Legaria 694, Irrigación, 11500, Miguel Hidalgo, CDMX, México.*

<sup>c.</sup> *Área de Química Aplicada, Departamento de Ciencias Básicas, Universidad Autónoma Metropolitana-Azcapotzalco, 02200, Ciudad de México, México*

<sup>d.</sup> *Departamento de Ingeniería de Procesos e Hidráulica, División de Ciencias Básicas e Ingeniería, Universidad Autónoma Metropolitana-Iztapalapa, 09340, Ciudad de México, México.*

<sup>e.</sup> *UNICAT, Departamento de Ingeniería Química, Facultad de Química, Universidad Nacional Autónoma de México, 04510 Ciudad de México, México.*

<sup>f.</sup> *Department of Chemistry, The University of Texas at Austin, Austin, Texas 78712, United States.*

<sup>g.</sup> *Departamento de Química, División de Ciencias Básicas e Ingeniería, Universidad Autónoma Metropolitana (UAM-I), 09340, México. Ricardo A. Peralta: Email: rperalta@izt.uam.mx.*

<sup>h.</sup> *Centro de Nanociencias y Nanotecnología, Universidad Nacional Autónoma de México, Km 107 Carretera Tijuana-Ensenada, Ensenada, B.C., C.P. 22800, Mexico.*

<sup>i.</sup> *On Sabbatical as “Catedra Dr. Douglas Hugh Everett” at Departamento de Química, Universidad Autónoma Metropolitana-Iztapalapa, Avenida San Rafael Atlixco 186, Leyes de Reforma Ira Sección, Iztapalapa, Ciudad de México 09310, México.*

<b>S1.</b>	<b>Experimental</b>	<b>details</b>
.....		<b>S3</b>
<b>S2.</b>	<b>Results</b>	<b>and</b>
.....		<b>S4</b>
<b>S3.</b>		<b>References</b>
.....		<b>S16</b>

## **S1. Experimental details**

### **Materials**

Bismuth (III) acetate ( $(\text{CH}_3\text{CO}_2)_3\text{Bi}$ , 99.99 %), Ellagic acid (HPLC  $\geq 95$  %), Acetic acid glacial ( $\text{CH}_3\text{CO}_2\text{H}$ , 99 %) were supplied by Sigma-Aldrich. All reagents, gases, and solvents were used as received from commercial suppliers without further purification.

### **Analytical instruments**

#### **Powder X-Ray Diffraction Patterns (PXRD)**

PXRD was recorded on a Rigaku Diffractometer, Ultima IV, with Cu-K $\alpha$ 1 radiation ( $\lambda = 1.5406$  Å) using a nickel filter. The patterns were recorded in the range 2–50° 2 $\theta$  with a step scan of 0.02° and a scan rate of 0.05° min<sup>-1</sup>.

#### **Fourier-transform infrared spectroscopy (FT-IR)**

FT-IR spectra were obtained in the range of 4000-500 cm<sup>-1</sup> on a Shimadzu IRTracer-100 spectrometer with a Golden Gate Single Reflection diamond ATR cell.

#### **Thermal gravimetric analysis (TGA)**

TGA was performed using a TA Instruments Q500HR analyzer under an N<sub>2</sub> atmosphere using the high-resolution mode (dynamic rate TGA) at a scan rate of 5 °C min<sup>-1</sup>, from room temperature to 800 °C.

#### **Solid-state ultraviolet-visible spectroscopy (UV-Vis)**

Absorption measurements were performed from 200-800 nm using a Shimadzu spectrophotometer UV-2600 equipped with an ISR-2600Plus integrating sphere and a BaSO<sub>4</sub> blank.

#### **X-ray Photoelectron Spectroscopy (XPS)**

It was conducted with a PHI VersaProbe 4 instrument using a nonmonochromatic Al K $\alpha$  source (1486.6 eV) and the charge neutralizer. The instrument's base pressure was  $\sim 10^{-9}$  torr. High-resolution spectra were collected over an analysis area of  $\sim 250 \times 250$   $\mu\text{m}^2$  using a pass energy of 10 eV. Binding energy was calibrated using the C 1s peak for adventitious hydrocarbons at 284.8 eV. Data analysis was performed using CasaXPS software.

## **S2. Results and Discussion**

### **Characterization of SU-101**

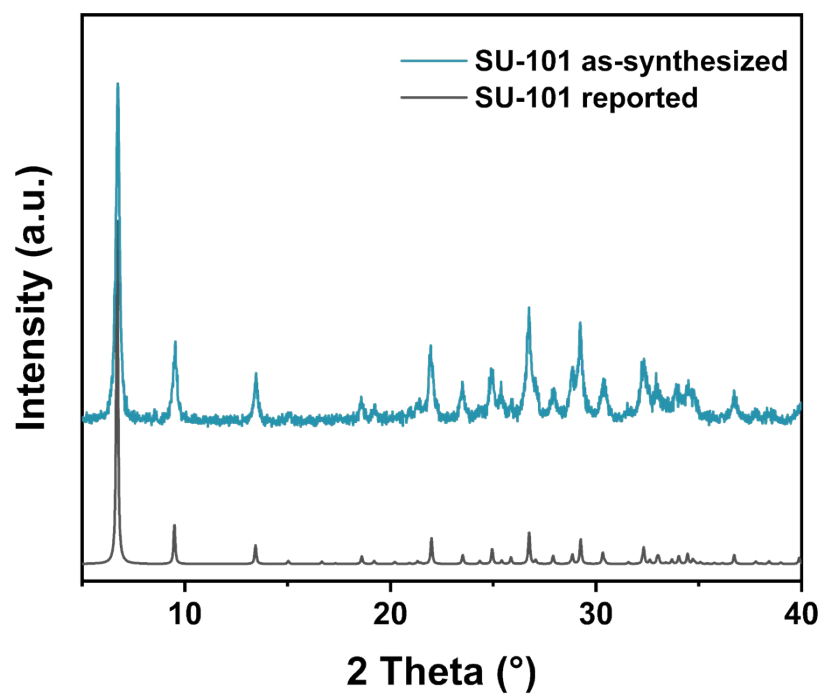


**Figure S1.** PXRD pattern of SU-101 reported and SU-101 as-synthesized

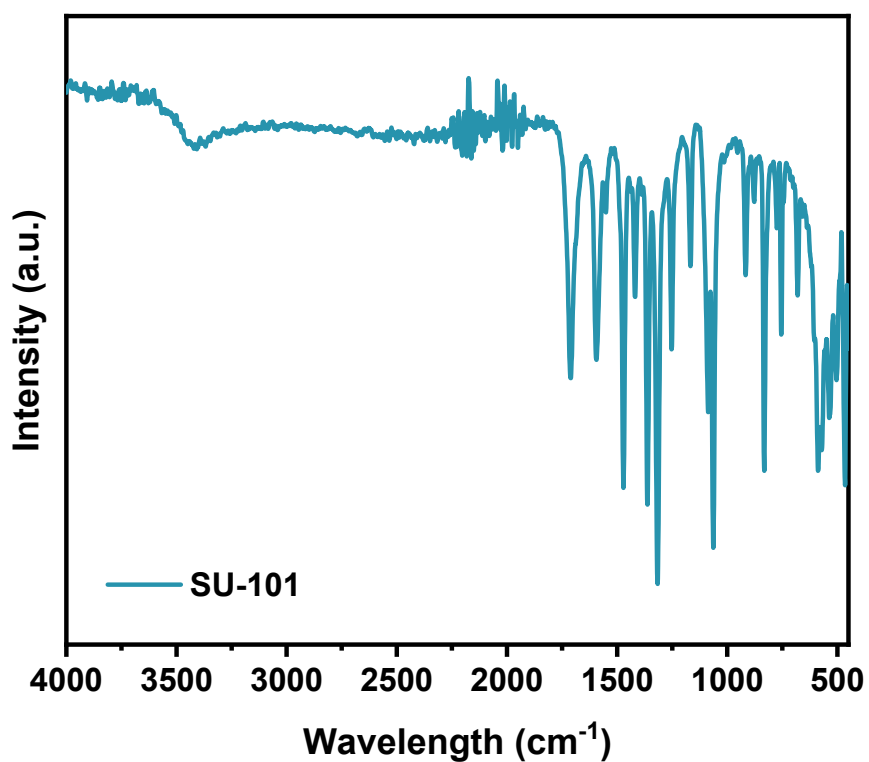


**Figure S2.** FTIR spectra of SU-101 as-synthesized.

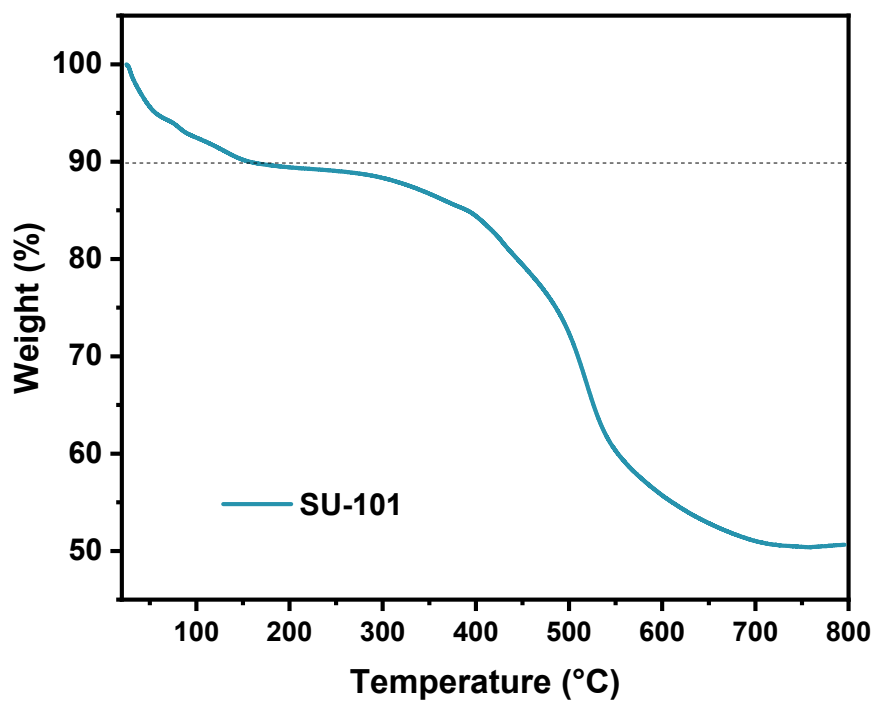


Figure S3. TGA profile of SU-101 as-synthesized.

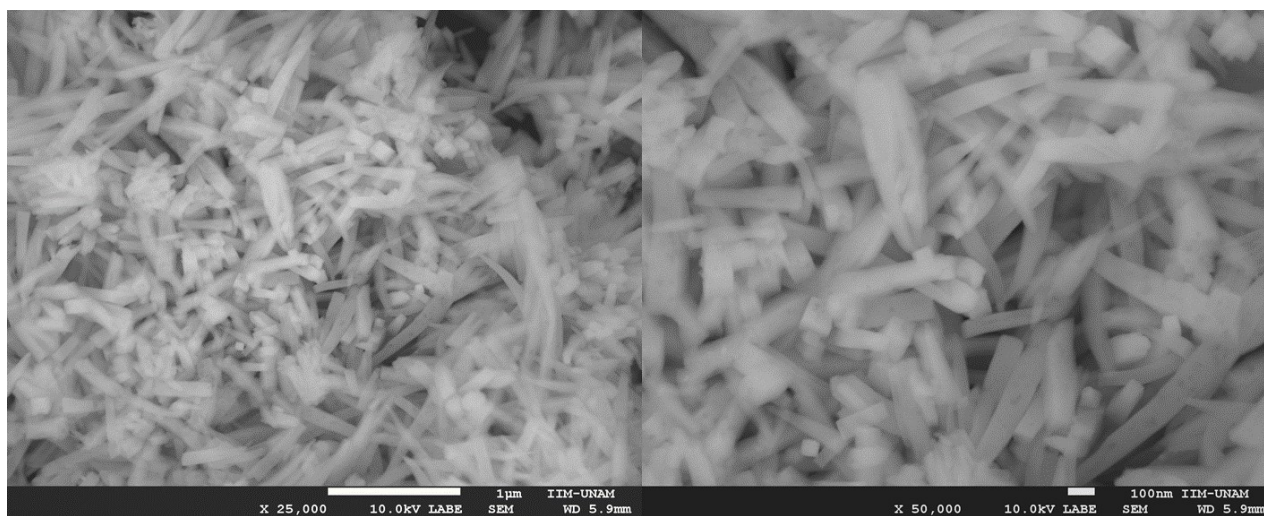


Figure S4. SEM images of SU-101 as-synthesized.

## H<sub>2</sub>S saturation experiments

The system (Figure S5) contains two principal parts:

- A. The gas generator, in which  $\text{Fe}_2\text{S}_3$  is added to a two-neck ball flask [1], one of which is capped with a rubber stopper through which concentrated HCl is injected with a glass syringe [2], while the other port is connected to the saturation chamber.
- B. The saturation chamber, made of a round flask [3], is connected to a vacuum line [4] and a vacuum line [4]. vacuum line [4] and a pressure gauge [5].

To start the process, a sample of about 15 mg in a 1.5 mL glass vial was activated in a sand bath with  $\text{N}_2$  flow at 120 °C under vacuum for 12 h. The vial was then placed in the saturation chamber, and the system was evacuated with a vacuum line. Next,  $\text{H}_2\text{S}$  gas was generated by dripping concentrated HCl over  $\text{Fe}_2\text{S}_3$ , the sample was left continuously exposed to the gas for 3 hours.

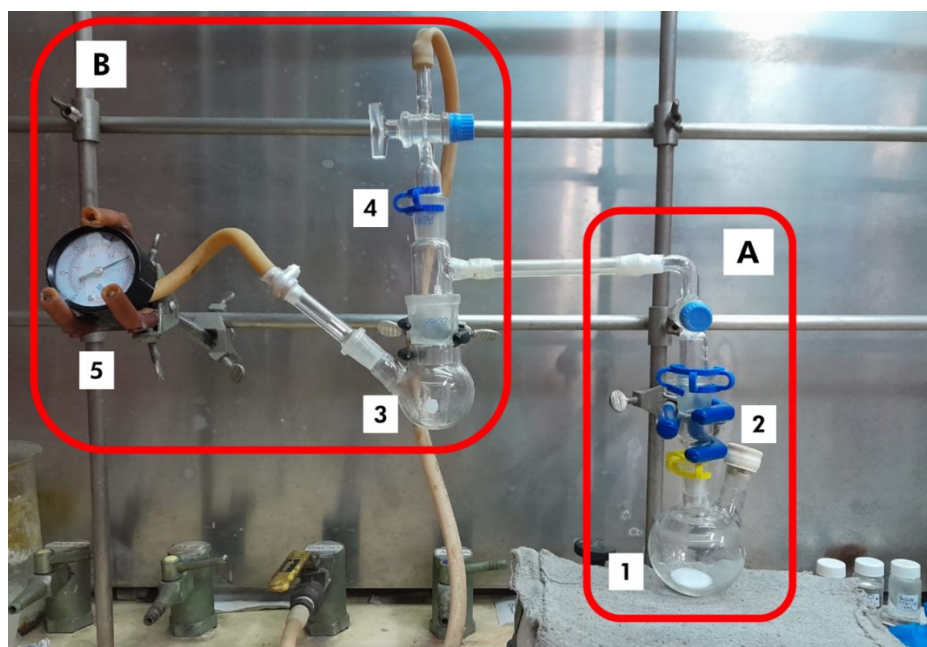


**Figure S5.** *in-situ*  $\text{H}_2\text{S}$  homemade system.

## **$\text{H}_2\text{S}$ breakthrough experiments**

$\text{H}_2\text{S}$  experiments were made using a HP 5890 GC, by continuous injections of the system exhaust, of each injection we obtained a chromatogram. From the corresponding chromatogram

we integrate the H<sub>2</sub>S signal to obtain its quantity. Knowing the H<sub>2</sub>S concentration from the feed, we can calculate the H<sub>2</sub>S concentration in each one of the injections, as the saturation concentration is the original feed concentration. Dynamic breakthrough experiments were carried out in a home-made system.

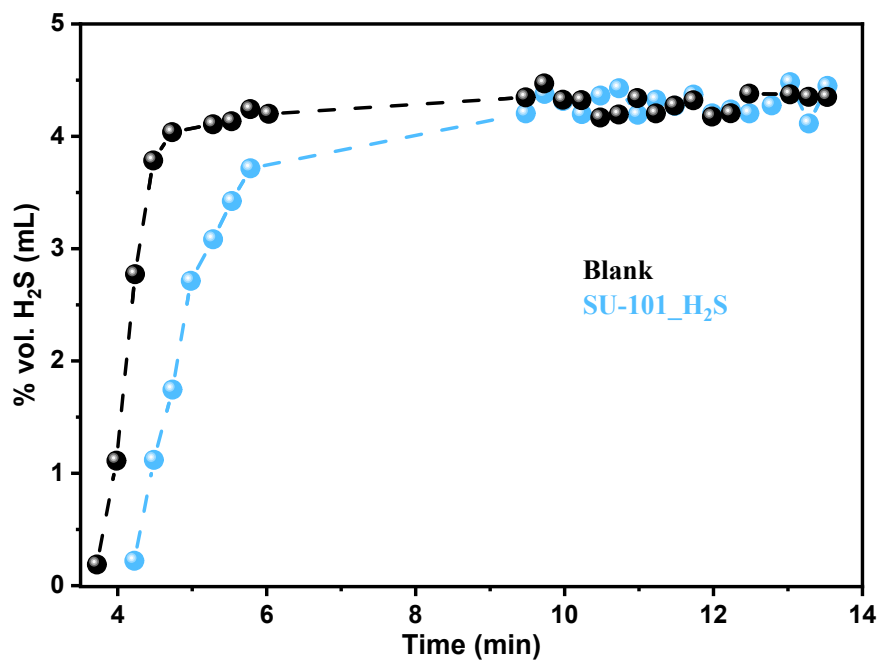


**Figure S6.** Breakthrough curve of H<sub>2</sub>S adsorption by SU-101 at 25 °C and 1 bar.

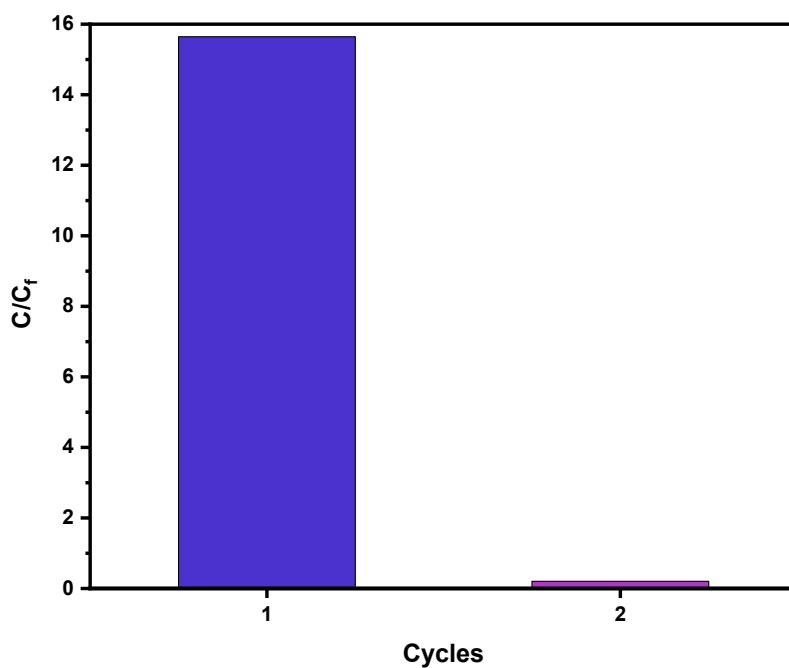


**Figure S7.** Comparative H<sub>2</sub>S adsorption capacities for two cycles.

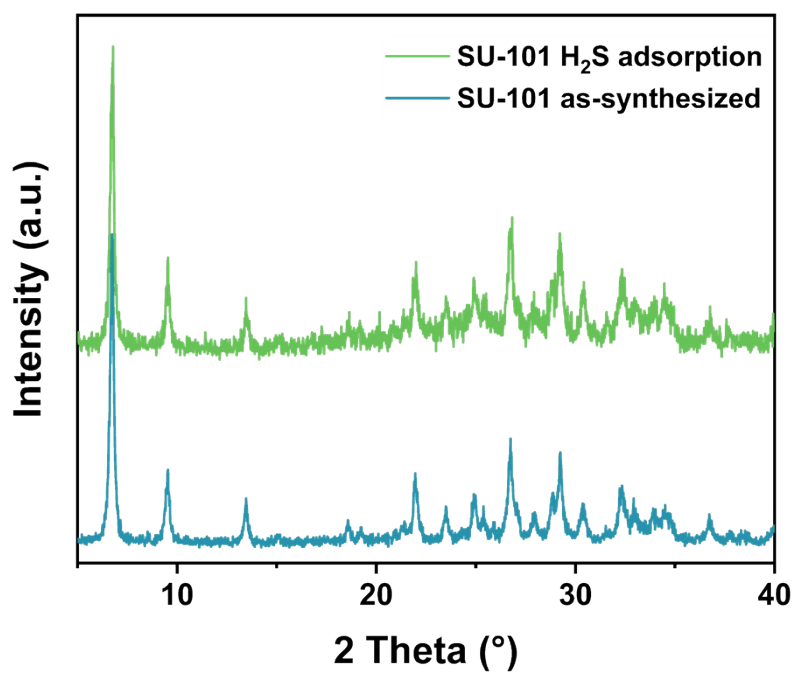


**Figure S8.** PXRD patterns of SU-101 as-synthesized and SU-101 after H<sub>2</sub>S adsorption.

<b>Table S1.</b> Evolution of SU-101 as a function of contact time with H <sub>2</sub> S, quantifiable in GC.		
Time (s)	H <sub>2</sub> S uptake (mmol g <sup>-1</sup> )	Image
120	0.00	
145	0.06	
170	0.15	

195	0.24			
220	0.33			
245	0.44			
270	0.46			
670	0.73			

**Fluorescence experiments**

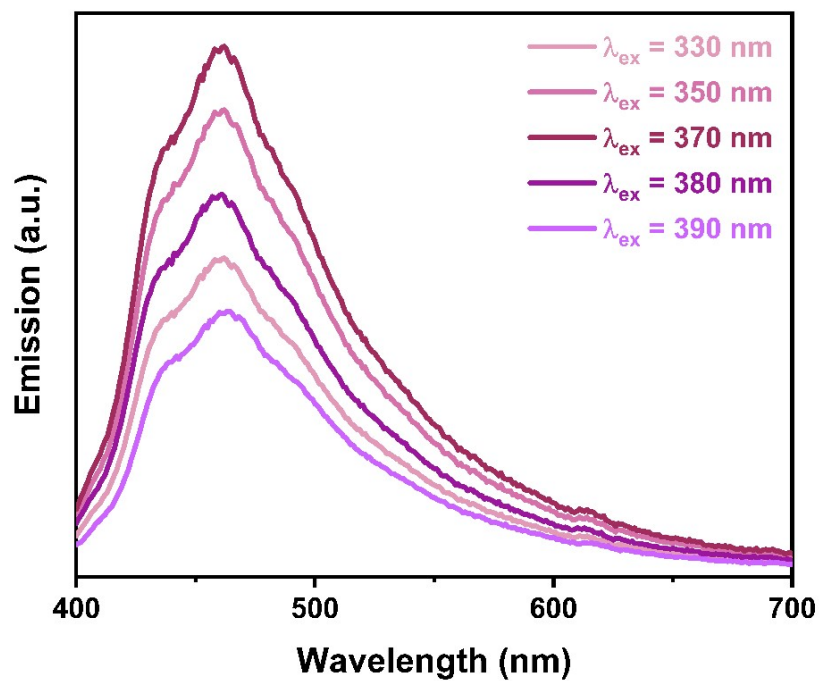


**Figure S9.** Solid-state emission spectra of activated SU-101 at different excitation wavelengths.

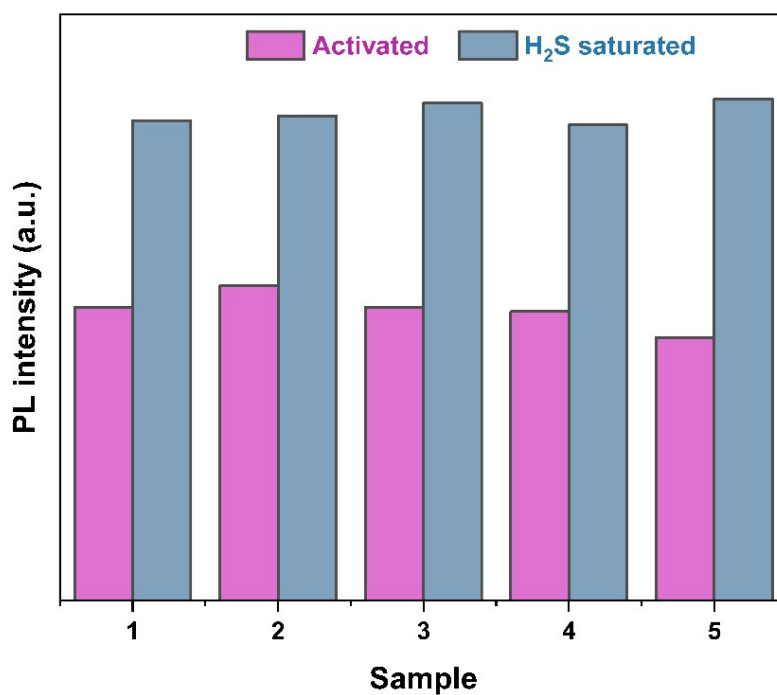


**Figure S10.** Fluorescence emission of five independent samples activated and saturated with H<sub>2</sub>S.

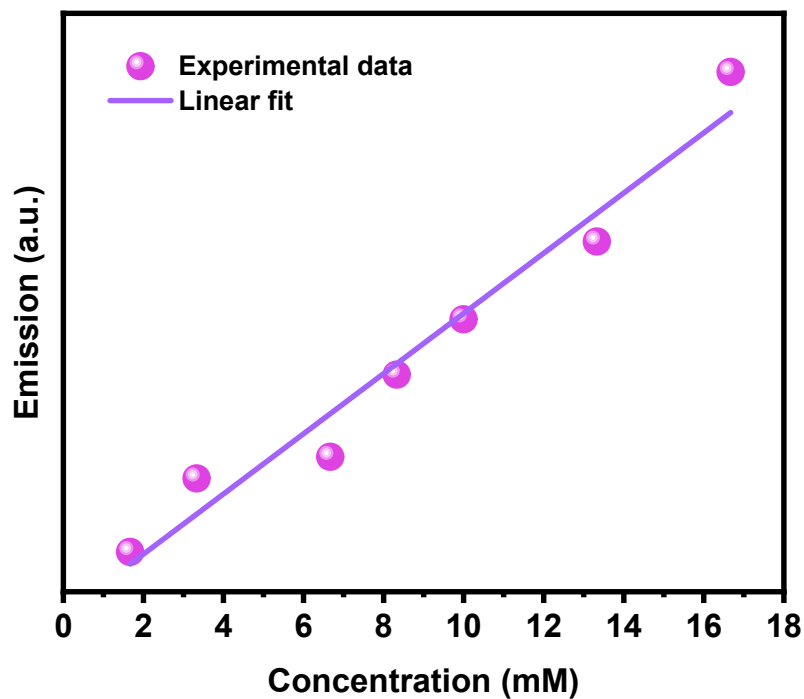


Figure S11. Determination of LOD.

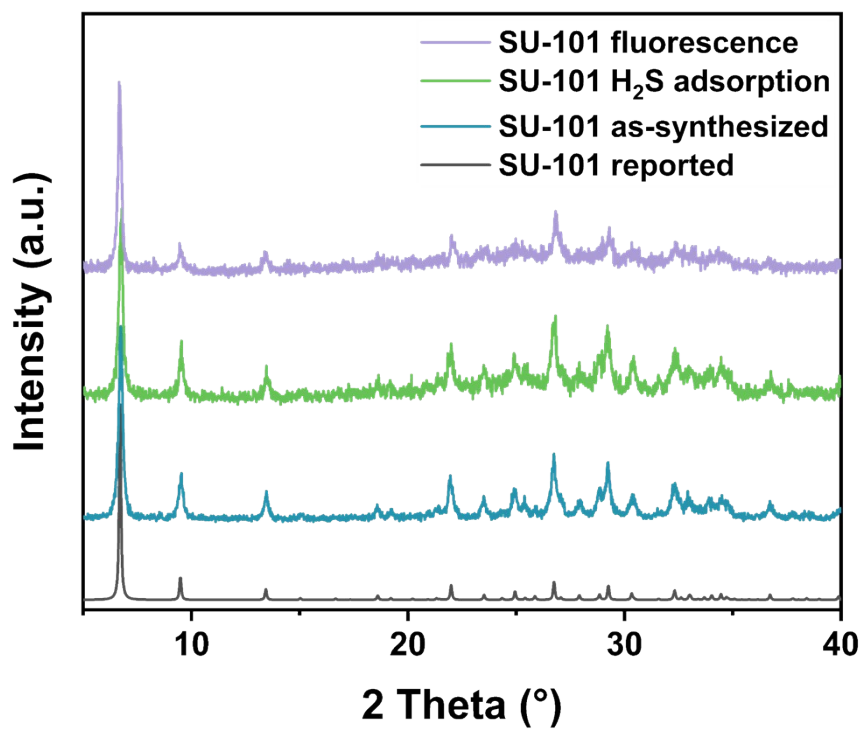


Figure S12. PXRD patterns of SU-101 reported, as-synthesized, after H<sub>2</sub>S in our home-made in situ device, and after the fluorescence test.

## Tauc plots for the determination of the energies between HOMO-LUMO orbitals by direct and indirect method

The determination of the energy between the HOMO-LUMO orbitals of the activated and H<sub>2</sub>S-saturated SU-101 material, were performed by constructing Tauc plots using solid-state UV-visible spectroscopy data.<sup>S2</sup> Tauc plots in Figure S13, allow the assessment of the type of electronic transition present, either a direct or indirect transition, based on the analysis of the optical absorption of the material.

The following relationships were used for this assessment:

- Direct transitions:  $(\alpha h\nu)^2 \propto (h\nu - E_{gap})$
- Indirect transitions:  $(\alpha h\nu)^{\frac{1}{2}} \propto (h\nu - E_{gap})$

Where  $\alpha$  is the absorption coefficient,  $h\nu$  is the photon energy, and  $E_{gap}$  represents the HOMO-LUMO energy gap. By extrapolating the linear region of the Tauc plot to  $\alpha=0$ , the  $E_{gap}$  value for each transition type is obtained.

The values obtained for the direct and indirect transitions are shown in Table S2.

**Table S2.** HOMO-LUMO energy values considering direct and indirect transitions calculated from the Tauc method for the activated, and H<sub>2</sub>S-saturated SU-101 samples.

Sample	Direct (eV)	Indirect (eV)
SU-101 activated	2.32	2.20
H <sub>2</sub> S saturated	1.83	1.73

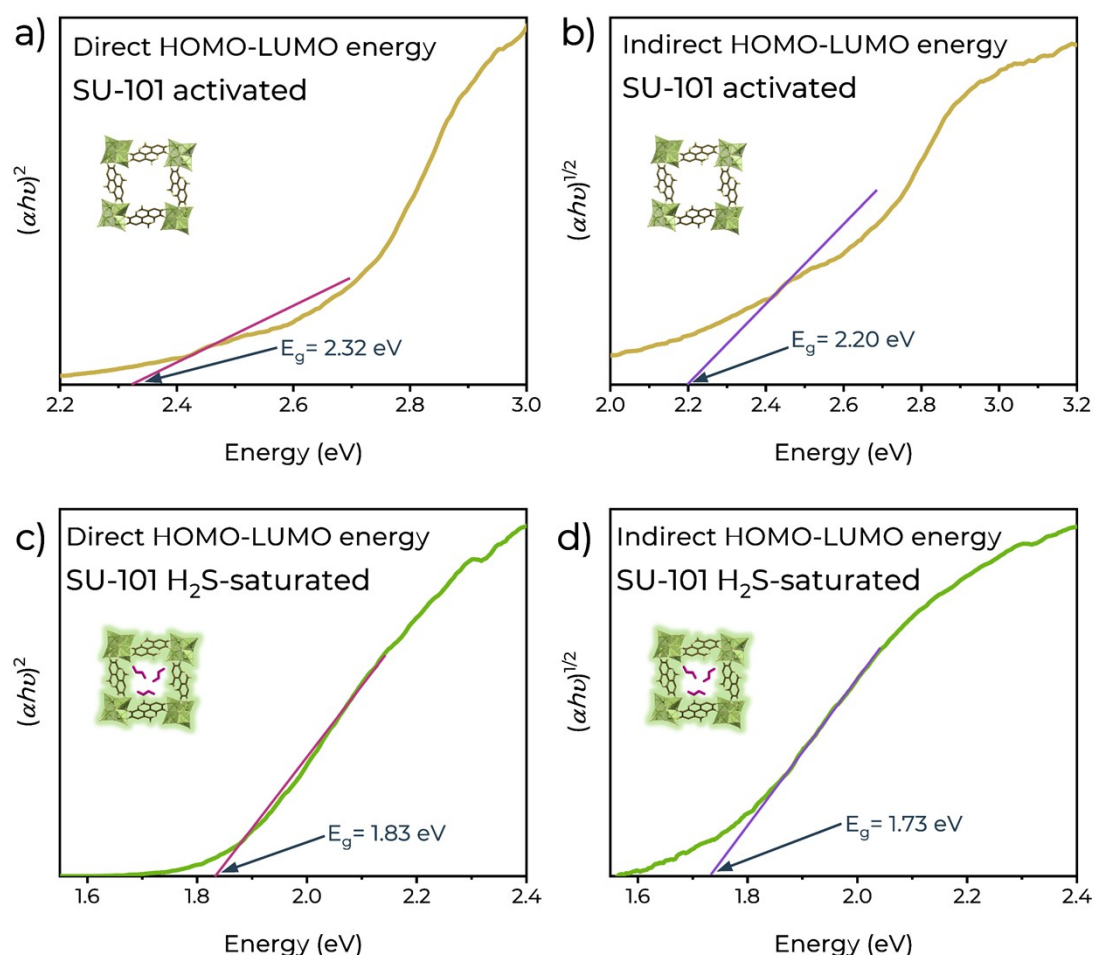


**Figure S13.** Tauc plots considering direct and indirect transitions for (a) and (b) activated SU-101 (yellow), and (c) and (d) saturated with H<sub>2</sub>S (green).

### TRPL experiments

Fluorescence lifetimes were determined from the TPRL spectra. The data obtained from the decay spectra were fitted in Fluoracle software, using a multi-exponential equation (Equation 1) to describe the fluorescence emission decay curve:<sup>S3</sup>

$$R(t) = B_1 e^{\left(\frac{-t}{\tau_1}\right)} + B_2 e^{\left(\frac{-t}{\tau_2}\right)} + B_3 e^{\left(\frac{t}{\tau_3}\right)} + B_4 e^{\left(\frac{-t}{\tau_4}\right)}$$

where R(t) represents the fluorescence intensity as a function of time, B<sub>1</sub>, B<sub>2</sub>, B<sub>3</sub> and B<sub>4</sub> are the amplitudes of the respective decay components, and τ<sub>1</sub>, τ<sub>2</sub>, τ<sub>3</sub> and τ<sub>4</sub> are the lifetimes of the different components.

**Table S3.** Lifetimes of the activated and saturated samples.

SU-101	τ <sub>1</sub> (ns)	a <sub>1</sub>	τ <sub>2</sub> (ns)	a <sub>2</sub>	τ <sub>3</sub> (ns)	a <sub>3</sub>	τ <sub>4</sub> (ns)	a <sub>4</sub>	Lifetime (ns)
Activated	0.0866	0.1896	0.8685	0.3415	2.1830	0.3678	7.9120	0.1011	<b>1.9158</b>
H <sub>2</sub> S saturated	0.0597	0.0548	1.1787	0.3744	2.8721	0.4138	8.2971	0.1570	<b>2.9357</b>

## Electronic structure calculations

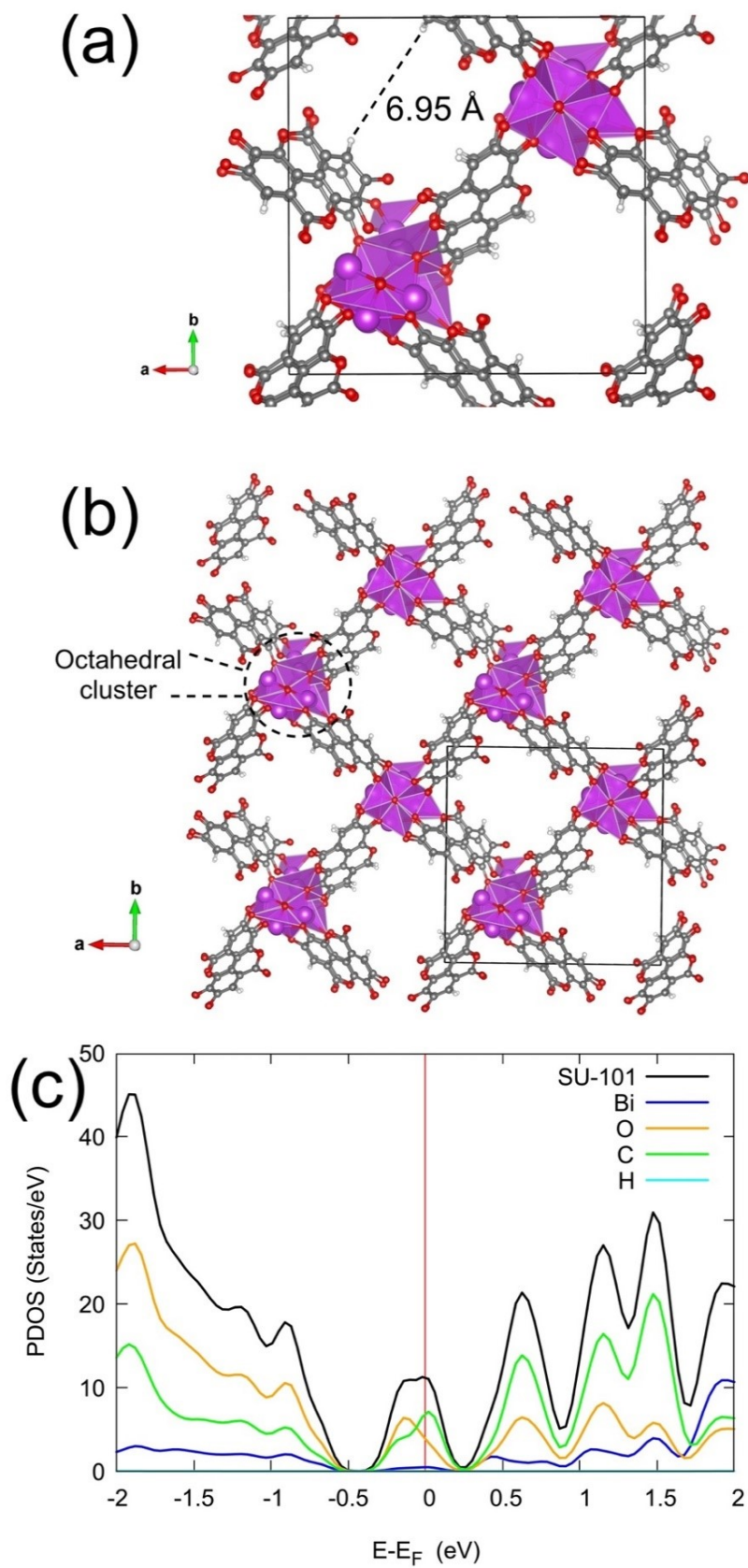


**Figure S13.** (a). The supercell 2 x 2 relaxed, (b) periodic conditions perspective of SU-101 crystal structure, and (c) partial density of states (PDOS) of SU-101 structure.

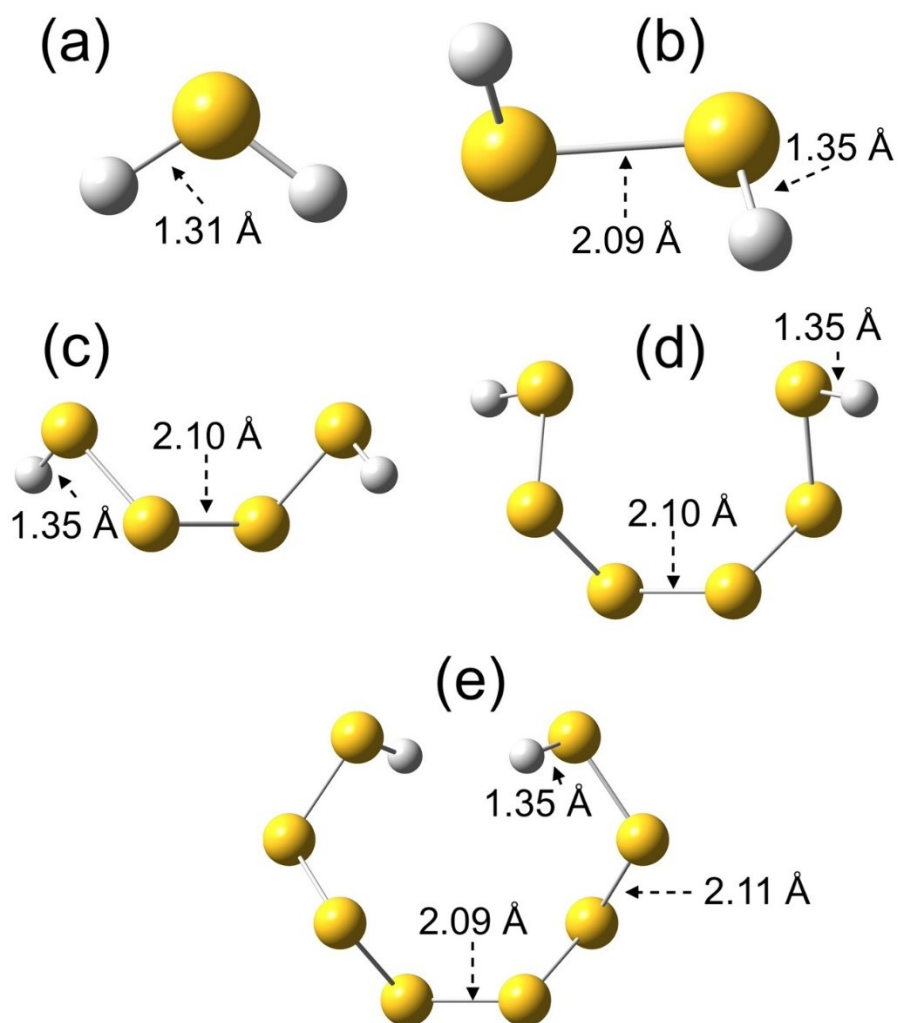


**Figure S14.** Optimized geometries corresponding of (a)  $\text{H}_2\text{S}$  molecule and polysulfide species to (b)  $\text{H}_2\text{S}_2$ , (c)  $\text{H}_2\text{S}_4$  (d) $\text{H}_2\text{S}_6$ , (e)  $\text{H}_2\text{S}_8$ .

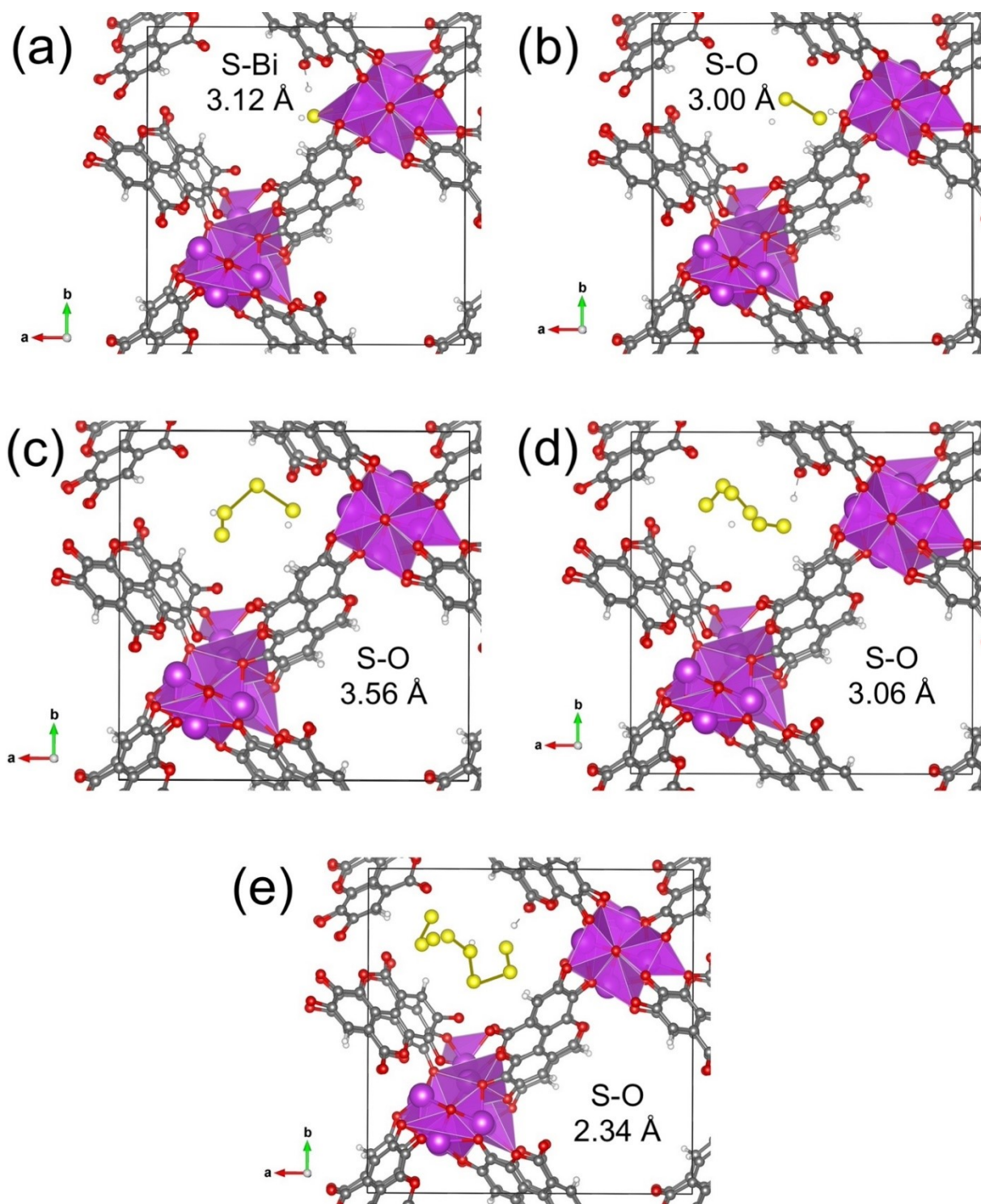


**Figure S15.** Optimized geometries corresponding  $\text{H}_2\text{S}$  molecule and polysulfide interaction into SU-101 structure: (a)  $\text{H}_2\text{S}/\text{SU-101}$ , (b)  $\text{H}_2\text{S}_2/\text{SU-101}$ , (c)  $\text{H}_2\text{S}_4/\text{SU-101}$ , (d)  $\text{H}_2\text{S}_6/\text{SU-101}$ , (e)  $\text{H}_2\text{S}_8/\text{SU-101}$ .

**Table S4.** Adsorption energies ( $E_{\text{ads}}$ ) given in the interaction of the SU-101 structure interacting with  $\text{H}_2\text{S}$  molecule and polysulfide under study.

System	$E_{\text{ads}}$ (eV)
$\text{H}_2\text{S}/\text{SU-101}$	-1.30
$\text{H}_2\text{S}_2/\text{SU-101}$	-1.50
$\text{H}_2\text{S}_4/\text{SU-101}$	-0.87
$\text{H}_2\text{S}_6/\text{SU-101}$	-1.01
$\text{H}_2\text{S}_8/\text{SU-101}$	-1.78

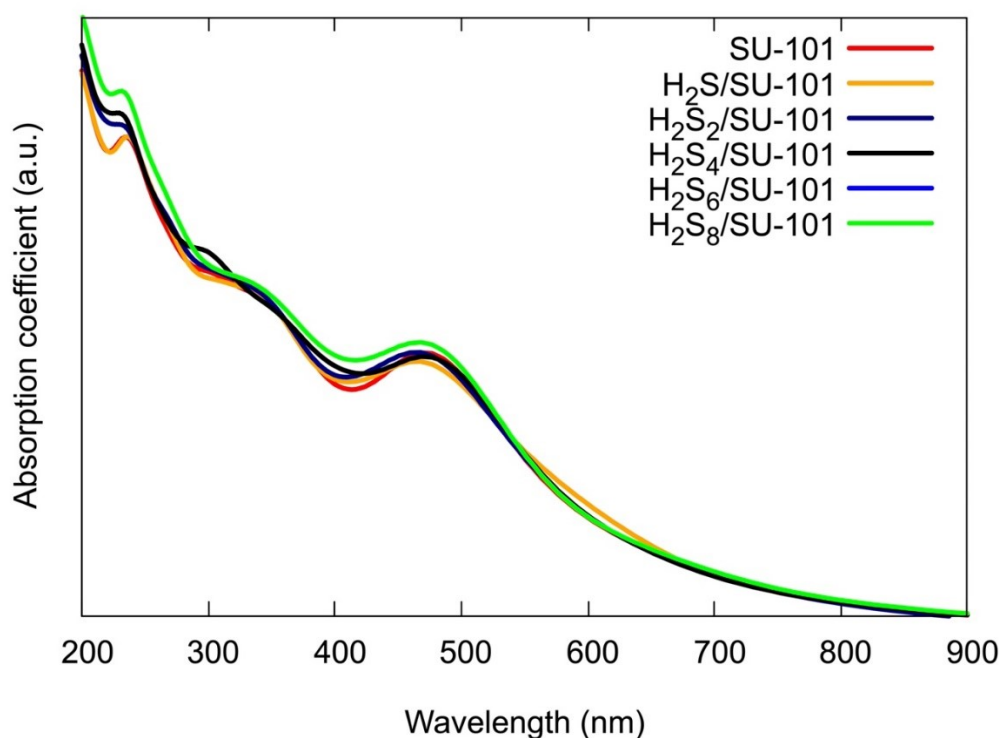


**Figure S16.** Simulated absorption spectra of the SU-101 structure interacting with  $\text{H}_2\text{S}$  molecule and polysulfide under study.

### S3. References

- (1) Grape, E. S.; Flores, J. G.; Hidalgo, T.; Martínez-Ahumada, E.; Gutiérrez-Alejandre, A.; Hautier, A.; Williams, D. R.; O’Keeffe, M.; Öhrström, L.; Willhammar, T.; Horcajada, P.; Ibarra, I. A.; Inge, A. K. A Robust and Biocompatible Bismuth Ellagate MOF Synthesized Under Green Ambient Conditions. *J. Am. Chem. Soc.* **2020**, *142* (39), 16795–16804. <https://doi.org/10.1021/jacs.0c07525>.
- (2) P. H. M. Andrade, C. Volkringer, T. Loiseau, A. Tejada, M. Hureau and A. Moissette, *Appl. Mater. Today*, 2024, *37*, 102094.
- (3) U. Noomnarm and R. M. Clegg, *Photosynth. Res.*, 2009, *101*, 181–194.